Gearbox loads caused by double contact simulated with HAWC2

Hansen, Anders Melchior; Rasmussen, Flemming; Larsen, Torben J.

Published in:
Proceedings

Publication date:
2011

Document Version
Publisher's PDF, also known as Version of record

Gearbox loads caused by double contact simulated with HAWC2

Anders M. Hansen[†], Flemming Rasmussen[†], Torben J. Larsen[†]
[†]Wind Energy Department, Risø-DTU, DK-4000 Roskilde, Denmark
anmh@risoe.dtu.dk

"EWEC conference 2011, Brussels"

1 Abstract

The aim of the work presented in this paper is to investigate if a special event named "double contact" between individual gear wheels inside a gear box can be the cause for some of the frequent occurrences of gearbox failures experienced in modern wind turbines. The investigation is made by interfacing a simulation model of the dynamic behaviour of a gearbox to the aeroelastic code HAWC2. The response of the coupled simulation models are then analysed in order to see if and under which circumstances the double contact event occurs and which loads are achieved inside the gearbox.

The paper introduces first the double contact hypothesis as motivation for the study. Then the generalised interface to HAWC2 is described which is used to couple the gearbox model and the wind turbine model in HAWC2. The simulation model of the gearbox is then described and the gearbox model and the wind turbine model are joined and the coupled response is obtained and analysed with special attention to the double contact event. Finally, conclusions are made.

2 Double contact theory

Even though gearboxes using planetary stages have been used for centuries, the drive train layout normally used in wind turbines, see Figure 1, has special design features, which might cause problems not seen in other planetary stage applications. Apart from the torque transfer from low speed side to high speed side, the gear box also works as a second main bearing of the main shaft. Hereby all force reactions from the rotor as well as the gravity and inertial loads from the gear box itself will be transferred through the main bearings between carrier and housing down to the gear box suspension normally consisting of two rubber bushing arrangements. A special and important feature of the planetary gear is the load alleviating effect of the floating sun-wheel suspension. This floating sun-wheel suspension allows for small movements of the sun-wheel, which ensures an excellent load distribution between the three planets. The theory of this section is that the load transfer through the main bearings can be influenced by a double contact situation inside the planetary stage if an unfortunate ratio between bearing clearance and teeth clearance occurs.

A double contact is a situation where the tooth is in normal contact on the driving side and at the same time in contact on the back side as illustrated in Figure 3. Such a double contact situation is not considered a problem if it only occurs between one set of planet-sun and planet-ring teeth connections, but in the case where double contact on two sets of planet-sun and planet-ring connections occurs simultaneously a completely changed load sharing between the planet wheels occurs. The reason for the changed load sharing during a double-contact is that the two planet wheels involved with the double-contact makes a small rotation which forces the sun-wheel to be in contact with only these two planets. The third planet is then completely unloaded which causes the input torque to be taken by two instead of three planets causing an increased load at the teeth and bearings during this moment of contact.

In the quest for the explanation of the many gear box failures especially seen in the period from 1995 to 2005, the dynamics of the traditional drive train layout, has previously been investigated. In a research project funded by the Danish Energy Agency, a dynamical model of the drive train arrangement was modeled by Larsen et. al [1],[2]. In this model the main components in the drive train was modeled using a lumped spring/mass approach coupled to a 2D spring mass model of the planetary stage, originally formulated by Lin and Parker [3]. The drive train model is illustrated in Figure 2. The tooth contact in the planetary stage illustrated in Figure 2 is modeled using linear springs for the tooth flexibility and lumped inertia for the wheel bodies. The main results from that investigation was that the load alleviating effect of the floating sun-wheel suspension together with the limited inertia of the sun-wheel caused a very fine load distribution in all investigated load cases. Another result of the investigation was that the inertia of the gear box mounted on the main shaft and gear stay suspension through a carrier that was surprisingly flexible caused vibration modes mainly dominated by the gear box translation with frequencies down to 10Hz, which is in the frequency range of the aerodynamic input loads. However, the analysis did not give a reason for the gear box failures. One limitation of the analysis was that the drive train model was not coupled to the rest of the turbine.

The behaviour of the planetary gear stage was further investigated by Parker et al.[4]. The focus of this analysis was directly on the double contact situation. The model used for the analysis was again the original model by Lin and Parker, [3], but now also equipped with extra non-linear springs representing the clearance between the teeth and inside the bearings and an extra set of springs for the double contact, see Figure 3. In this analysis performed with constant input torque and gravity loading it was clearly seen that a change in loads occurred. A load increase for the planetary bearings by a factor of 1.75 is seen in Figure 4.

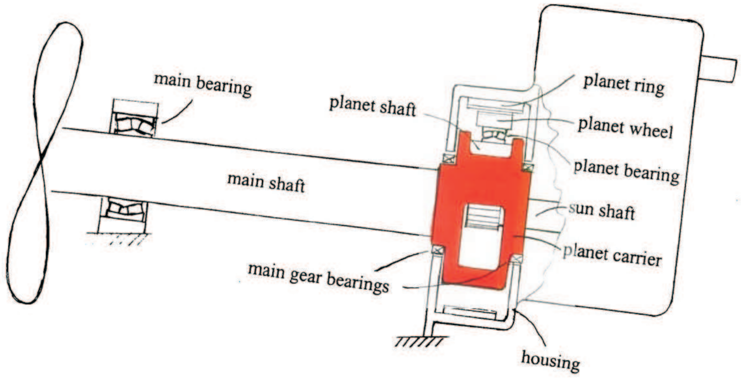

Figure 1: Traditional layout of wind turbine drive train. The gear box which consists of a planetary stage and two parallel stages also works as the second main bearing on the main shaft.

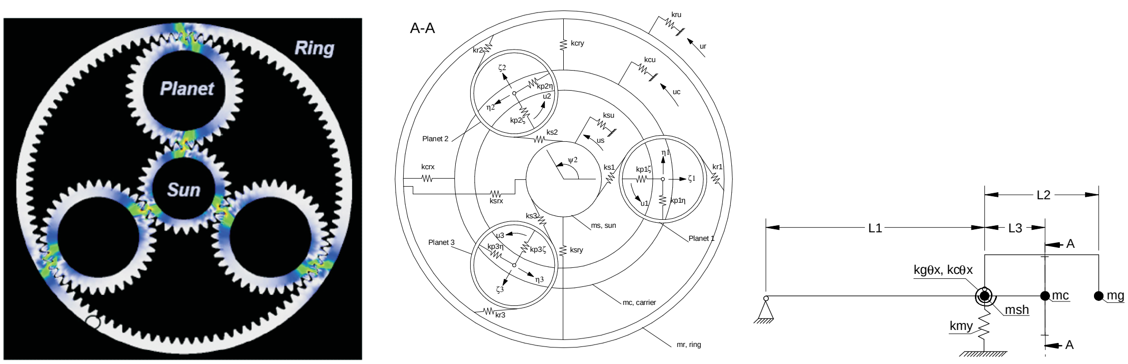

Figure 2: Left: Compression forces in a normal tooth contact situation of a planetary gear stage. Right: Dynamical model used to investigate the drive train dynamics with particular focus on gear teeth and bearing forces.

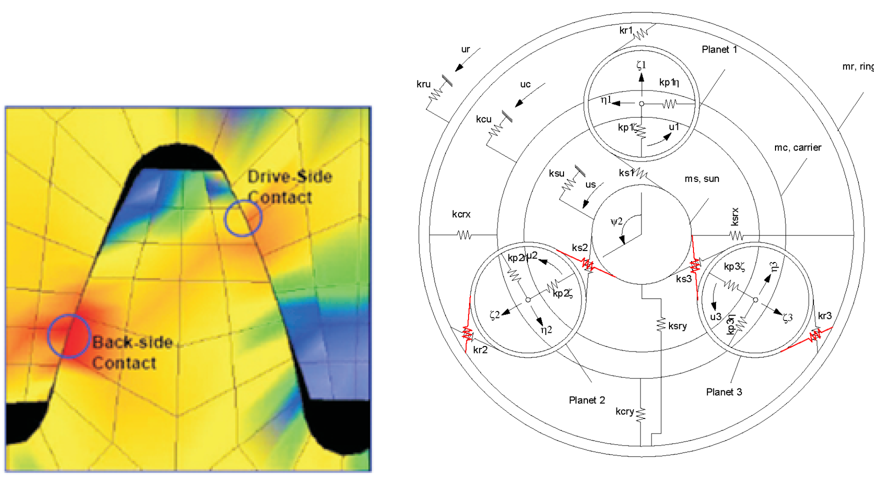

Figure 3: Left: Example of a double contact situation where the backside of the teeth are also in contact. Right: Double contact springs inserted (with red). Springs are non-linear and only active during compression. Only double contact spring is illustrated for the two lower planets even though they are also present for the upper planet.

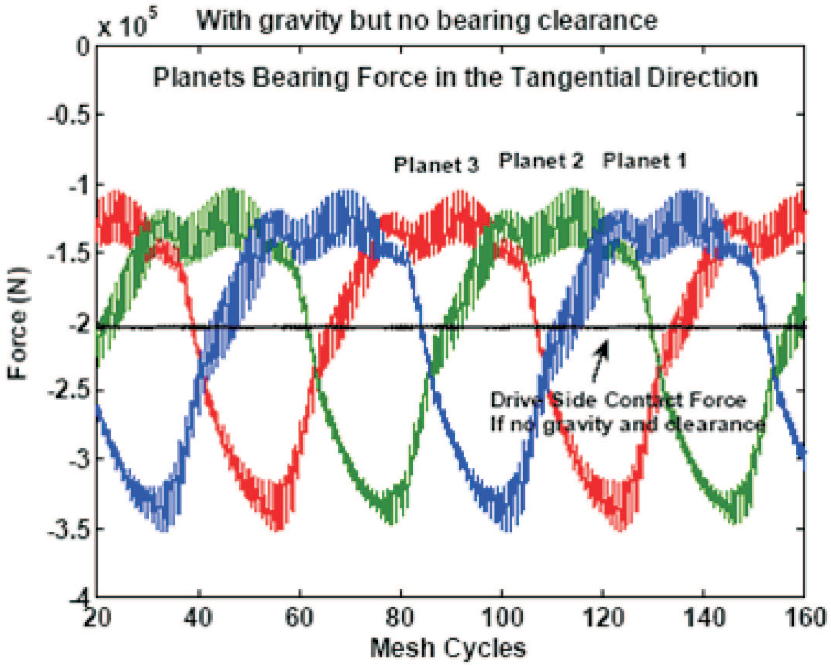

Figure 4: Preliminary analysis of the double-contact situation. It can be seen that planet forces are highly un-equal depending on the azimuth position during a double-contact situation even though the input torque is constant.

3 The solution of externally formulated equations of motions together with the HAWC2 core DOFs

The gearbox model used for this paper uses a new interface which enables externally formulated equations of motions to be solved together with the core equations of motions in the HAWC2 code.

The external system interact with the HAWC2 model through a set of constraint equations which describes how the external system degrees of freedom (DOFs) and the HAWC2 DOFs are related. Both the EOMs for the external system and the constraint equations are specified in an external DLL which is then called by the HAWC2 solver during the simulation.

In order for HAWC2 to be able to solve the combined EOMs, the external system DLL must return some specific information to HAWC2. To understand what is required by the DLL, it is useful to explain how the EOMs are formulated in HAWC2. The basic assumption is that the EOMs for the external system can be formulated by use of some kind of variational principle, such as e.g. the Virtual Work Principle or Hamiltons Principle - if so, the sum of virtual work, δW, for the internal (i.e. the HAWC2 system, subscript i) and external system (subscript e) is:

$$\delta W = \delta W_i + \delta W_e = \delta \mathbf{q_i} \cdot \mathbf{B_i} + \delta \mathbf{q_e} \cdot \mathbf{B_e} = 0$$

In the 2nd last part of the equation above, the virtual work is expressed as a function of the virtual DOFs, $\delta \mathbf{q_i}$ and $\delta \mathbf{q_e}$ for the internal and external DOFs, respectively. The virtual work must be zero for the systems to be in equilibrium for all the virtual variations of the DOFs which requires the vectors $\mathbf{B_i}$ and $\mathbf{B_e}$ to be equal to $\mathbf{0}$. (Note that if the external system is a simple mass/damper/spring system with external forces acting on it, then
$\mathbf{B_e} = \mathbf{M} \cdot \ddot{\mathbf{q_e}} + \mathbf{C} \cdot \dot{\mathbf{q_e}} + \mathbf{K} \cdot \mathbf{q_e} - \mathbf{F}$

The vectors $\mathbf{B_i}$ and $\mathbf{B_e}$ express the un-constrained EOMs for the systems. The systems are not interacting with each other since they do not share any DOFs. If somehow the systems were constrained to move in a certain manner relative to each other, we would have to introduce external forces acting on both systems in order to obtain the constrained movement of the systems. This is done by introducing the Lagrange Multiplier Method, cf. [5], which adds some extra virtual energy to the system virtual energy necessary to satisfy the constraints. The constrained movement between the systems are formulated in a set of constraint equations gathered in the constraint vector $\mathbf{g}(\mathbf{q_i}, \mathbf{q_e}) = \mathbf{0}$. For each constraint equation, a new DOF (called a Lagrange multiplier) is introduced and collected in the vector λ. Now the virtual constraint energy is added to the system virtual energy, like this

$$\begin{aligned}
0 &= \delta W + \delta(\lambda \cdot \mathbf{g}) \\
&= \delta W + \delta\lambda \cdot \mathbf{g} + \delta \mathbf{g} \cdot \lambda \\
&= \delta \mathbf{q_i} \cdot \left(\mathbf{B_i} + (\nabla_{q_i} \mathbf{g})^T \cdot \lambda\right) + \delta \mathbf{q_e} \cdot \left(\mathbf{B_e} + (\nabla_{q_e} \mathbf{g})^T \cdot \lambda\right) + \delta\lambda \cdot \mathbf{g} \\
&= \delta \mathbf{q_i} \cdot (\mathbf{B_i} + \mathbf{G_i} \cdot \lambda) + \delta \mathbf{q_e} \cdot (\mathbf{B_e} + \mathbf{G_e} \cdot \lambda) + \delta\lambda \cdot \mathbf{g}, \quad \forall \delta \mathbf{q_e},\ \forall \delta \mathbf{q_i},\ \forall \delta\lambda
\end{aligned}$$

The last line in the equation above introduces the gradient matrices $\mathbf{G_e}$ and $\mathbf{G_i}$ (or rather the transpose of that), which contain the derivatives of the constraint vector wrt. $\mathbf{q_e}$ and $\mathbf{q_i}$, respectively. Since the total virtual energy must be zero for all virtual variations of the DOFs, we finally get these EOMs:

$$\mathbf{B_i} + \mathbf{G_i} \cdot \lambda = \mathbf{0}$$

$$\mathbf{B_e} + \mathbf{G_e} \cdot \lambda = \mathbf{0}$$

$$\mathbf{g} = \mathbf{0}$$

It is now clear which tasks the external DLL needs to do in order to couple an external system with the HAWC2 model:

- The un-constrained EOMs for the external system, $\mathbf{B_e}$, need to be formulated, along with
- the constraint vector, $\mathbf{g}$, and the gradient matrices, $\mathbf{G_e}$ and $\mathbf{G_i}$.

The two bulleted tasks above are really not dependent and they can be specified separately in external DLLs, providing the possibility to do simulations of external systems without constraining them to any internal systems. Also, constraints between internal systems can be defined without having to introduce an external systems. Further, which is not really clear from the description above, it is also possible to specify constraints between individual external systems, so that it is possible to couple two (or more) external systems together.

4 Gearbox model

The gearbox model was formulated with the aim of providing a flexible tool to model all kinds of gearboxes, both parallel and planetary gear stages and multiple stages as well. This was achieved by setting up the dynamic equations for a single gear wheel in a floating frame of reference giving each gear wheel 12 degrees of freedom - 6 for the floating frame and 6 for local displacements and rotations inside the floating frame (see Figure 5). The gear wheels can subsequently be grouped so that they share the same floating frame of reference.

$$\mathbf{r}_i(t) = \mathbf{R}(t) + \mathbf{A}(t) \cdot \left(\mathbf{R_0^i} + \mathbf{A_1^i} \cdot \mathbf{u}_i(t) + \mathbf{A_2^i}(t) \cdot \mathbf{x}_i\right)$$

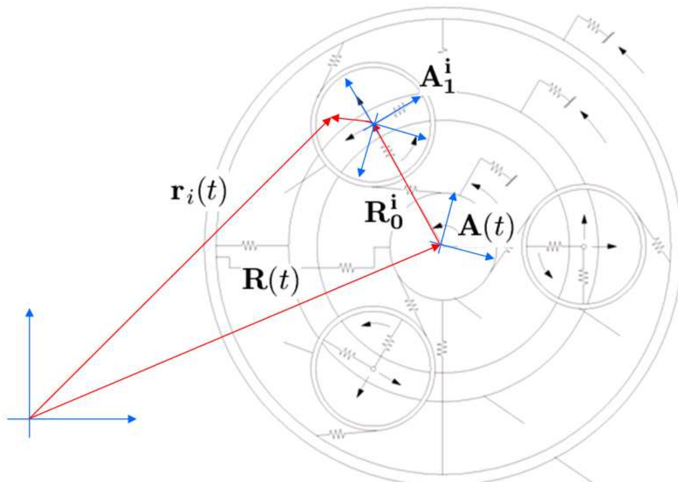

Figure 5: The figure shows kinematics of a single gear wheel, here one of the planet wheels. The displacement of the floating frame of reference is given by the vector $\mathbf{R}(t)$ and the rotation is given by the rotation matrix $\mathbf{A}(t)$. The wheel offset is defined by $\mathbf{R_0^i}$ and the orientation of the local displacements of the wheel is defined by the rotation matrix $\mathbf{A_1^i}$. The local displacement and rotation are described by $\mathbf{u_i}(t)$ and $\mathbf{A_2^i}(t)$, respectively.

Springs can be defined related to the local DOFs. Further, springs and dampers between groups of gear wheels can be modelled with external force models combined with appropriate constraint equations. Normally such springs are introduced to model bearing stiffness. A dead band can also be defined for the springs in order to model bearing clearance.

The model of the gear tooth interaction is modeled by a spring/damper model combined with an appropriate constraint equation which accounts for the relative movement between interacting gear teeth. The force model is defined so that it only allows pressure forces to occur between the individual gear teeth. Furthermore, a dead band can be defined in order to model backlash.

5 Coupled analysis

In this section the combined aeroelastic response of the gearbox and the wind turbine during operation in turbulent wind is analysed with special attention to the double contact event.

For the present turbine, the shaft is supported by two bearings, one near the rotor (front) and another embedded in the gear box (rear). The force reaction at the rear bearing perpendicular to the shaft is mainly composed of a constant contribution from the gravity on the rotor and a time varying contribution from the aerodynamic loading on the rotor. The time varying load is generated when the blades pass the fluctuations in wind speed (due to wind shear, tower shadow, and turbulence) over the rotor disc and therefore there will be orientations relative to the blades which are loaded more than others. Since the location of the planets are fixed relative to the blades, one should expect the initial mounting of the rotor relative to the planets in the gearbox (at least for the 1st gear stage) to be of importance. This hypothesis is also investigated.

The three Figures 6, 7, and 8 show results from an aeroelastic simulation with the same input parameters, i.e. same turbine model (600kW stall regulated), same mean wind (10m/s) and same turbulence time series. Only the gearbox models differ. The turbine is started at low rotor RPM and the generator is cut out. After approximately 12 sec. the rotor has reached the cut-in speed and the generator is activated. The four graphs in each plot show the gear tooth reaction forces on planet wheel #1 between *sun/planet* and *ring/planet* on the *front* side and *back* side of the tooth, respectively.

The results shown in Figure 6 is the reference case with no clearance in the main bearing. In this case the forces on the end of the shaft perpendicular to the shaft are supported by the main bearing. The variation in tooth forces are caused by variations in wind speed and hence the torque transmitted through the gearbox. No tooth forces on the back side of the gear teeth are observed which means that the gear box operates as intended without any double contact events occurring.

The gearbox used to generate the results in Figure 7 has low main bearing stiffness so that the forces on the shaft end are no longer supported by the main bearing. Instead the force is supported by the interaction between the planet and the ring causing double contact between the gear teeth and increased tooth forces.

The results shown in Figure 8 demonstrate the significance of how the rotor is mounted relative to the planets in the gearbox. In this case the rotor and gearbox are rotated 60deg relative to the position used for the results in Figure 7, but otherwise the two gearboxes are identical. The tooth forces are seen to be larger in this case which indicates that an optimum relative rotation between rotor and gearbox exists which minimizes the tooth forces in case of double contact.

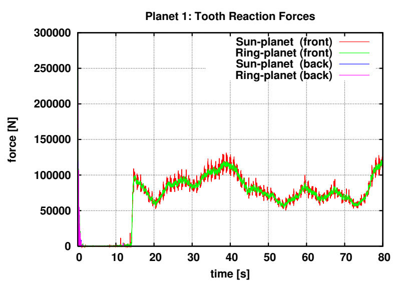

Figure 6: Normal operation case without double contact. The variation in loading is caused by turbulent wind speed variation.

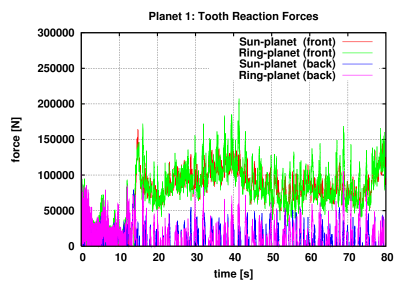

Figure 7: Large carrier bearing clearance is applied which causes double contact. Loads are increased significantly. The rotor is mounted so that the three planets are aligned with a blade.

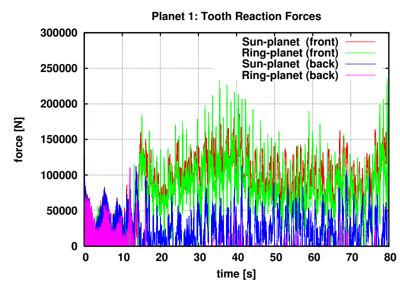

Figure 8: Same gearbox as the one to the left, but the mounting of the gearbox relative to the blades is rotated 60deg. This results in an even larger load increase.

5.1 Conclusion

The coupled dynamic response of the gearbox and wind turbine was investigated during operation in turbulent wind with special emphasis on the double contact hypothesis. Three simulations were run in which only the gear box differed. The differences in the responses were investigated and the following conclusions are made.

High clearance in the planet carrier bearings in combination with low tooth clearance (backlash) increases the risk of double contact. If this occurs, the internal forces on teeth and planetary bearings are significantly increased due to an uneven load sharing between the planets. In this condition the radial forces transferred between the planetary wheels and the ring are approximately added directly to the planet bearing forces in the driving direction and not as a square root sum, as one might expect.

The additional planet bearing loads originating from the rotor bending moments are dependent upon how the three planets in the gearbox are positioned relative to the three blades with a maximum depending upon turbine characteristics. This might contribute to the explanation of gearbox failures seen in the past and explain the variability in failures of apparently identical turbines as the mounting azimuth position is random.

References

[1] T. J. Larsen, K. Thomsen, and F. Rasmussen. Dynamics of a wind turbine planetary gear stage. In *Proceedings CD-ROM. CD 2. European wind energy conference and exhibition 2003 (EWEC 2003)*. EWEA, 2003.

[2] T. J. Larsen, K. Thomsen, and F. Rasmussen. Dynamics of a wind turbine planetary gear stage. Technical Report Risø-I-2112(EN), Risoe, National Laboratory, 2003.

[3] J. Lin and Parker R. G. Analytical Characterization of the Unique Properties of Planetary Gear Free Vibration. *Journal of Vibration and Acoustics*, vol. 121:pp. 316–321, 1999.

[4] R. Parker, F. Rasmussen, and T. J. Larsen. Dynamic Modelling and Analysis of a Wind Turbine Planetary Gear with Tooth Backlash and Bearing Clearance. In *Poster presentation (EWEC 2006)*. EWEA, 2006.

[5] Ted Belytschko, Wing Kam Liu, and Brian Moran. *Nonlinear Finite Elements for Continua and Structures*. John Wiley & Sons Ltd., 2000.